

DOWN SYNDROME

Hedgehog Agonist Therapy Corrects Structural and Cognitive Deficits in a Down Syndrome Mouse Model

Ishita Das,¹ Joo-Min Park,^{2,3} Jung H. Shin,⁴ Soo Kyeong Jeon,² Hernan Lorenzi,^{1*} David J. Linden,² Paul F. Worley,² Roger H. Reeves^{1†}

Down syndrome (DS) is among the most frequent genetic causes of intellectual disability, and ameliorating this deficit is a major goal in support of people with trisomy 21. The Ts65Dn mouse recapitulates some major brain structural and behavioral phenotypes of DS, including reduced size and cellularity of the cerebellum and learning deficits associated with the hippocampus. We show that a single treatment of newborn mice with the Sonic hedgehog pathway agonist SAG 1.1 (SAG) results in normal cerebellar morphology in adults. Further, SAG treatment at birth rescued phenotypes associated with hippocampal deficits that occur in untreated adult Ts65Dn mice. This treatment resulted in behavioral improvements and normalized performance in the Morris water maze task for learning and memory. SAG treatment also produced physiological effects and partially rescued both *N*-methyl-D-aspartate (NMDA) receptor-dependent synaptic plasticity and NMDA/AMPA receptor ratio, physiological measures associated with memory. These outcomes confirm an important role for the hedgehog pathway in cerebellar development and raise the possibility for its direct influence in hippocampal function. The positive results from this approach suggest a possible direction for therapeutic intervention to improve cognitive function for this population.

INTRODUCTION

Trisomy for human chromosome 21 (Hsa21) results in Down syndrome (DS), which is among the most complex genetic conditions compatible with survival past term (1). Mouse models with segmental trisomy for orthologs of Hsa21 genes show a number of complex outcomes with regard to development and function that are relevant to DS (2). A phenotype-based approach made possible by these animal models has supported progress in understanding many outcomes of trisomy and has led to the development of therapeutic interventions (3–6).

The cerebellum is much smaller and hypocellular in people with DS (7), and in the Ts65Dn and other mouse models (8, 9). A hallmark of the Ts65Dn cerebellum, reduced density of granule cell neuron (GC) cell bodies in the internal granule layer, also occurs in people with DS across the entire life span (8). A critical reason for the reduced number of cerebellar GC in trisomic adults is a substantial reduction in the rate of cell division of trisomic granule cell precursors (GCPs) in the first days after birth. This reduction has been related to a prolonged cell cycle and results at least in part from the attenuated response of trisomic GCP to the mitogenic effects of Sonic hedgehog (Shh) growth factor (10, 11), the major mitogen for this cell population (12–14). When we administered a Shh pathway agonist, known as SAG, subcutaneously to trisomic Ts65Dn mice on the day of birth, we observed increased proliferation of GCPs. This treatment normalized GCP number 6 days later (P6) when Ts65Dn mice normally have a significant deficit in this cell population (10). Despite the initial delay, the mitotic index of GCPs in untreated trisomic mice reached the same rate as in euploid animals by postnatal day 6 (P6).

SAG 1.1 (SAG) is a derivative of chlorobenzo[*b*]thiophene, which was identified as a Shh pathway agonist (15, 16). SAG binds to and activates Smo, thus up-regulating the canonical Shh pathway and reproducing many activities of Shh *in vitro*. It is a small molecule that crosses the gut, the placenta, and the blood-brain barrier (10, 16, 17). SAG has been shown to stimulate division of neurons in the subgranular zone of the dentate gyrus (DG) after oral administration to adult mice (18). SAG has recently been given to newborn mice to stimulate GCP division, thereby counteracting the inhibition of GCP proliferation caused by administration of glucocorticoids (17).

The cognitive impairment seen in Ts65Dn, the most widely studied mouse model of DS, arises because of structural and functional differences in the trisomic brain compared to euploid (2, 8, 19–23). Several potential therapeutic approaches converge on the hippocampus because of its central role in learning and memory, functions that are disrupted in mouse models and also in people with DS (24, 25). Ts65Dn mice are markedly impaired in learning and memory, as evidenced by their performance in the Morris water maze (MWM), and are quite different from euploid animals in the induction of long-term potentiation (LTP) in the CA1 and DG of the hippocampus (26–28).

Here, we asked whether the positive effects on cerebellar development of perinatal treatment with SAG would persist in adult trisomic mice and what this might imply as a model for therapy in DS.

RESULTS

SAG treatment at birth normalizes cerebellar structure in adult mice

We synthesized SAG as described (15) and compared its ability to stimulate proliferation of GCPs relative to dually lipidated Shh (Shh-Np) (fig. S1). Newborn pups were injected with SAG (20 µg/g). This dose successfully normalizes proliferation of GCP in Ts65Dn mice for the first week of life, stimulates the Shh pathway *in utero* when given orally to pregnant dams, and stimulates proliferation of cells in the DG in

¹Department of Physiology and Institute for Genetic Medicine, Johns Hopkins University School of Medicine, Baltimore, MD 21205, USA. ²Department of Neuroscience, Johns Hopkins University School of Medicine, Baltimore, MD 21205, USA. ³Department of Physiology, Jeju National University School of Medicine, Jeju 690-756, South Korea. ⁴Institute on Alcohol Abuse and Alcoholism, National Institutes of Health, Rockville, MD 20857, USA.

*Present address: The J. Craig Venter Institute, Rockville, MD 20850, USA.

†Corresponding author. E-mail: rreeves@jhmi.edu

young adult mice (10, 16, 18). A dose in the same range (14.0 to 25.2 $\mu\text{g}/\text{kg}$) induces maximum expression of a Gli-luciferase reporter of Shh pathway activity in the brain (17).

At about 16 weeks of age, we determined cerebellar area at the midline in sagittal sections and cerebellar GC density of SAG-injected Ts65Dn mice (TsSAG), euploid animals injected with vehicle (EuVeh), and vehicle-injected trisomic animals (TsVeh) (Fig. 1). Adult TsSAG mice that received a single injection of SAG on the day of birth had the same cross-sectional area and GC density as EuVeh, and both were significantly greater than TsVeh (Fig. 1, A to C, and table S1). We showed previously that a single dose of SAG given to euploid mice (EuSAG) at P0 did not significantly increase GCP number at P6 (10).

We and others have shown that the number of granule cells in DG is reduced in Ts65Dn mice as early as P6, an effect that persists through the first year of life and presumably beyond (20, 21). Adult DG cell number is also influenced by external factors, such as activity or nutrition (29, 30). Accordingly, we looked for acute SAG effects on proliferation in the DG by co-injecting 5-bromo-2'-deoxyuridine (BrdU) and SAG at P0 and analyzing cell number at P6. In contrast to the normalization of cerebellar granule cell number 6 days after injection of SAG (10), the DG deficit in Ts65Dn mice that received SAG treatment was not ameliorated (Fig. 1D). TsVeh and TsSAG mice were not different from each other, and both showed a lower rate of proliferation in DG after SAG and BrdU labeling than did EuVeh (Fig. 1D, fig. S2, and tables S2 and S3).

SAG does not normalize long-term depression from cerebellar Purkinje cells

We asked whether normalization of cerebellar morphology would affect the synaptic function of cerebellar circuits measured in brain slice preparations. Excitatory postsynaptic currents (EPSCs) were recorded from Purkinje cells in lobule III and in lobule IX (Fig. 2), because there are known differences in electrophysiological properties between these areas (31). Despite the pronounced morphological differences between the Ts65Dn and euploid cerebellum, we did not find differences in EPSC kinetics as indexed by rise time or decay tau in either lobule III or lobule IX (table S4).

As an index of release probability at presynaptic terminal of GCs, we measured EPSC paired-pulse ratios (PPRs). PPRs were significantly lower in trisomic mice than in euploid in both lobule III and lobule IX ($P = 0.0009$ and 0.0006 , respectively) (Fig. 2B and table S4). SAG treatment did not restore the PPR values in trisomic mice. The lower PPR values in Ts65Dn suggest that release probability is increased at these synapses. This is consistent with a recent report that cerebellar GCs (the cells of origin of the parallel fiber axons) in Ts65Dn mice show increased excitability and larger action potential amplitude (32). We did not find any significant differences in long-term depression (LTD) expression in either lobule III or lobule IX (table S4). SAG treatment of Ts65Dn mice resulted in more depression of EPSC after the induction of LTD ($P = 0.019$), but this was limited to lobule III. Accordingly, it is difficult to relate therapeutic actions of SAG to effects on LTD. SAG treatment of euploid mice significantly decreased the PPR values measured in lobule IX ($P = 0.005$), but did not affect any other parameters.

SAG normalizes performance in hippocampal but not prefrontal tasks

Ts65Dn mice have been tested in numerous open-field paradigms for hyperactivity and anxiety levels, with highly inconsistent results

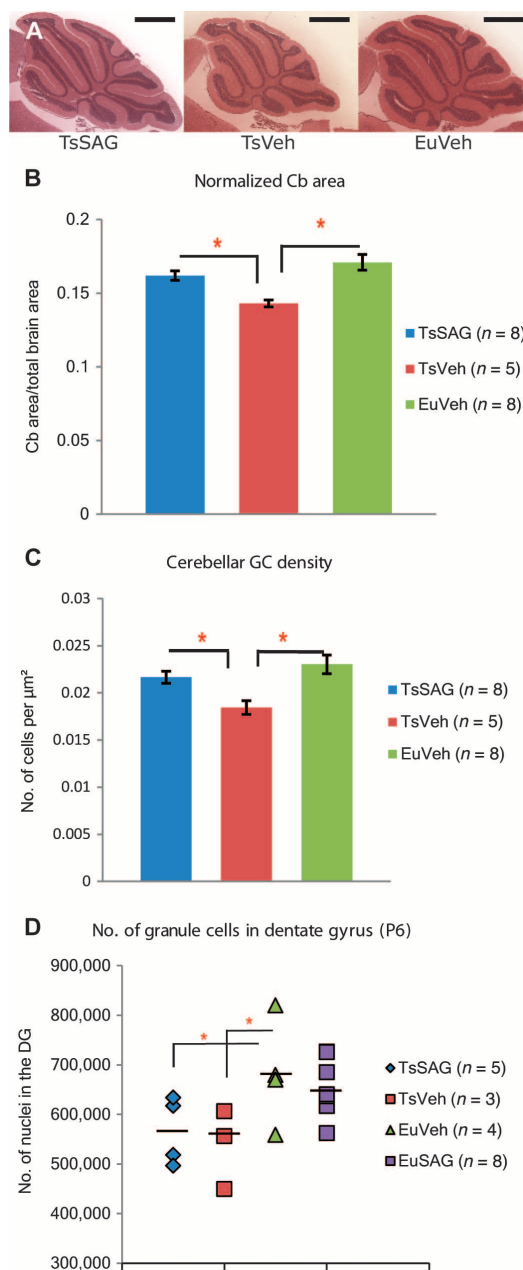


Fig. 1. An injection of SAG at P0 normalizes cerebellar morphology in adult Ts65Dn mice. (A) Representative sagittal images of TsSAG, TsVeh, and EuVeh cerebella, about 4 months of age. Hematoxylin and eosin. Scale bars, 1 mm. (B) Cerebellar (Cb) cross-sectional area is restored to euploid levels in TsSAG mice. Both TsSAG and EuVeh are significantly larger than TsVeh. (C) Cerebellar GC density is also restored in TsSAG mice. (B and C) Multivariate analysis of variance (MANOVA) for normalized cerebellar area and GC density, Wilk's $\lambda = 0.278$, $F = 0.583$, Fisher's LSD test; TsSAG versus TsVeh, $P = 0.02$; and TsVeh versus EuVeh, $P = 0.002$. (D) The number of granule cells in the DG at P6 was determined using stereology and showed no significant effect of SAG treatment (means indicated by a bar; TsSAG versus EuVeh: $P = 0.03$; TsVeh versus EuVeh: $P = 0.02$, Fisher's LSD for pairwise comparisons).

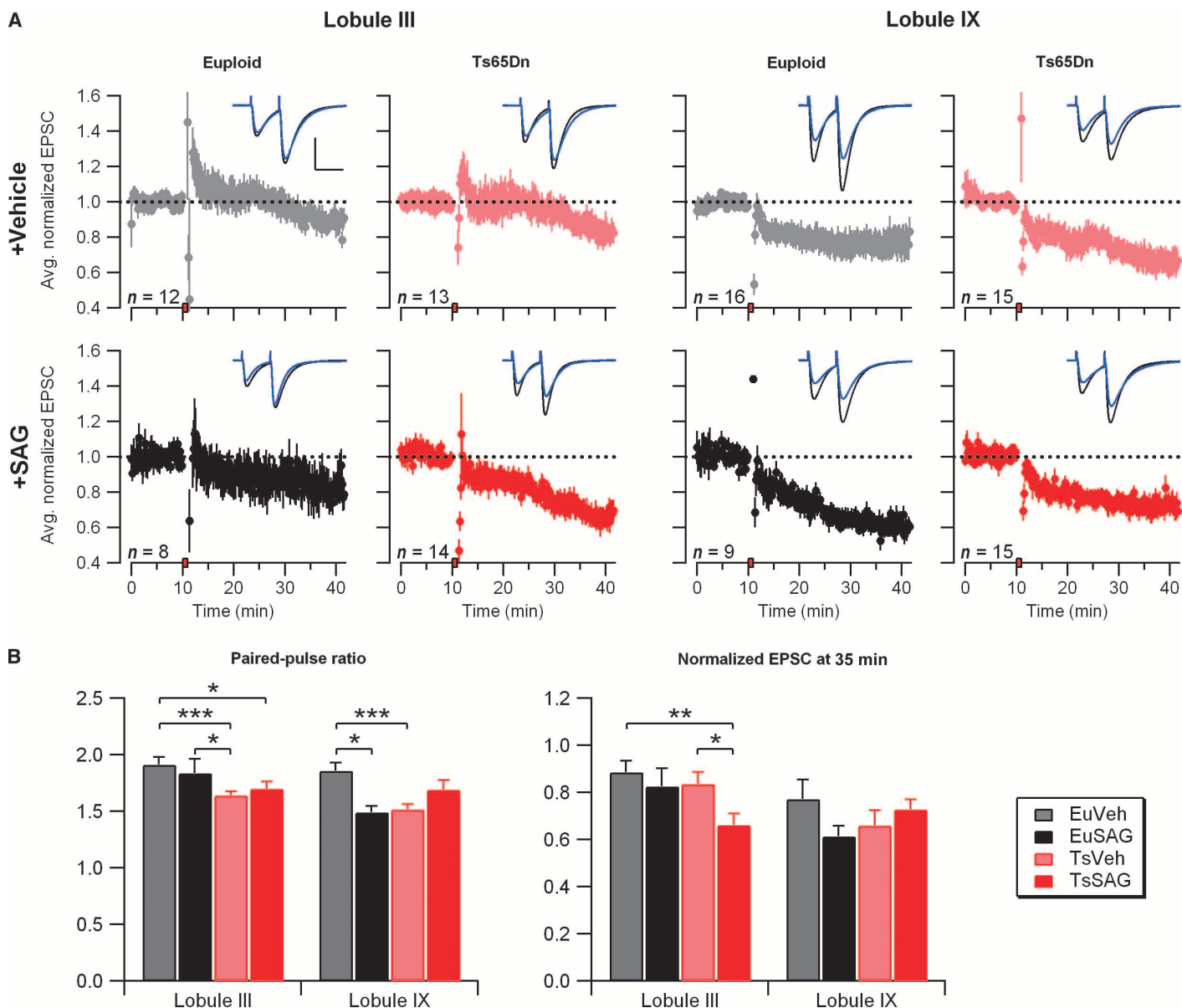


Fig. 2. Cerebellar LTD is minimally different between Ts65Dn and euploid mice. (A) Cerebellar LTD. EPSCs normalized to the baseline were averaged and plotted as a function of time for each group according to genotype (euploid or Ts65Dn), treatment (vehicle or SAG), and cerebellar lobule (III or IX). The red box on the x axis indicates the time of LTD induction. The error bars represent the SEM. The dashed line at 1.0 shows the

position of the baseline. Representative traces before (black) and 25 min after (blue) LTD induction ($t = 35$ min) are shown superimposed. Scale bars: 50 ms, 200 pA. (B) Bar graphs show the mean PPR measured at $t = 5$ min (before LTD induction) and normalized EPSC at $t = 35$ min (25 min after LTD induction). Exact P values for each measurement are in table S2. * $P < 0.05$, ** $P < 0.01$, *** $P < 0.001$.

[reviewed in (2)]. We used the open field to look for gross effects on general locomotor function while familiarizing the mice to handling. These procedures were not powered to detect small differences consistent with anxiolytic or anxiogenic effects (power is 60%). We found that the time spent in the periphery or center of the maze was similar for EuVeh and TsVeh groups, and no significant differences were observed with TsSAG (fig. S3). Separate measurements were made for the number of rearings and the number of beam breaks at the center or at the periphery, and these were further categorized into fine motor activity or ambulatory activity if the same beam was

broken twice or if consecutive beams were broken, respectively (fig. S3 and table S5).

Next, we assessed a previously described deficit of Ts65Dn in the Y maze test of working memory, a non-aversive task that does not involve training or a strong stimulus [see (2)]. EuVeh mice ($n = 13$) showed an average of 78% alternation. TsSAG and TsVeh mice were significantly impaired, with both groups showing only ~60% alternation [EuVeh versus TsSAG: $P = 0.003$; EuVeh versus TsVeh: $P = 0.0001$, Fisher's least significant difference (LSD)] (fig. S4A and table S6). With more power to detect differences in activity than in open field (about

85%), we observed significantly more activity, measured as number of arm entrances, in trisomic mice with or without SAG than in euploid mice (EuVeh versus TsSAG: $P = 0.001$; EuVeh versus TsVeh: $P = 0.002$, Fisher's LSD) (fig. S4B). SAG treatment did not have an effect on either outcome in Ts65Dn mice, nor did it alter outcomes in EuSAG compared to EuVeh.

Multiple investigators have reported that Ts65Dn mice display a robust deficit in hidden platform and probe component of the MWM task [summarized in (2)]. All four groups of mice tested here performed similarly in the visible platform component, as expected (Fig. 3A and table S7). Swimming velocities were not different between groups (fig. S5A). In the hidden platform paradigm, mice learn to navigate to the platform using visuospatial cues outside the tank. As expected, TsVeh mice had prolonged escape latencies compared to EuVeh. Bonferroni-corrected P values showed a significant difference between TsVeh and EuVeh in pairwise comparison (corrected $P = 0.003$). The pairwise comparisons were preceded by two-way repeated-measures ANOVA, which indicated a significant difference between the three groups ($F_{2,29} = 6.5$, $P = 0.005$, $\alpha = 0.05$). TsSAG mice had similar escape latencies as EuVeh mice ($P = 0.91$), and latencies for both groups were significantly shorter than those for TsVeh mice (TsSAG versus TsVeh, corrected $P = 0.042$) (Fig. 3B and table S8). The improvement in learning was also evident in the probe test (Fig. 3, C and D, and table S9) (Kruskal-Wallis rank test, $P = 0.001$; Mann-Whitney test for pairwise comparison, TsVeh versus TsSAG and TsVeh versus EuVeh, $P = 0.001$ and 0.0001 , respectively) and reflected improved memory in TsSAG mice compared to TsVeh (fig. S5). SAG treatment had no effect on the performance of euploid mice (Fig. 3).

We evaluated the strategy used to find the platform based on an analysis of trajectory and latency as described (33) (Supplementary Notes regarding behavior studies, fig. S5, B and C, and table S10). These parameters provide a detailed picture of spatial learning in the MWM that is not obtained from distance traveled alone. TsSAG mice used the same successful strategies as EuVeh, whereas the greatly increased latency for TsVeh mice was correlated with inefficient strategies. The strategy scores were highly correlated with latency in all three groups (Spearman's $\rho > 0.80$), indicating that time taken to find the platform was strongly related to the strategy.

Hippocampal physiology is partially normalized by SAG treatment

To determine whether improvements in MWM reflect physiological changes in the hippocampus, we used two different measures to characterize basal synaptic transmission. The first was to derive an index of synaptic strength by varying stimulus strength, thereby constructing an input-output plot relating presynaptic fiber volley (FV) amplitude to the onset slope of the field excitatory postsynaptic potential (fEPSP) (Fig. 4A and table S11). Second, we estimated the probability of neurotransmitter release by application of pulse pairs delivered at intervals ranging from 30 to 150 ms. The PPR serves as an index of release probability in a synapse (Fig. 4B and table S12). Both of these measures revealed similar basal synaptic properties in EuVeh, TsVeh, and TsSAG mice.

LTP evoked by theta burst stimulation (TBS) results in a rapid and sustained increase of AMPA receptor (AMPA)-mediated responses in Schaffer collateral-CA1 synapses (34). In hippocampal slices derived from EuVeh mice, fEPSP was increased to $138.6 \pm 3.4\%$ ($n = 12$) of baseline at $t = 30$ min after stimulation and sustained at the level of

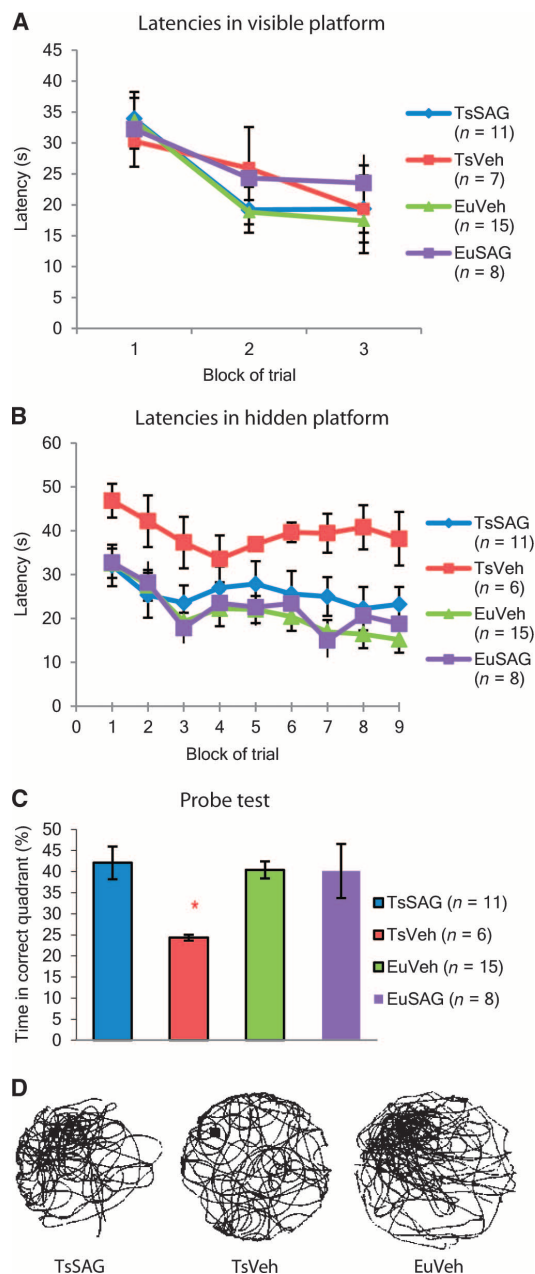


Fig. 3. SAG corrects performance of trisomic mice in tasks dependent on hippocampus. (A) TsVeh performed like EuVeh in MWM visible platform test, and there was no difference between TsVeh and TsSAG mice. Two-way repeated-measures ANOVA. (B) Latencies in the MWM hidden platform test were significantly longer in TsVeh than in EuVeh or TsSAG (two-way repeated-measures ANOVA, $F_{2,29} = 6.5$, $P = 0.005$, $\alpha = 0.05$). Bonferroni-corrected P values showed a significant difference between TsVeh and both TsSAG ($P = 0.003$) and EuVeh ($P = 0.042$), whereas TsSAG mice performed similarly to EuVeh ($P = 0.91$). (C) In the probe test, EuVeh and TsSAG mice spent significantly more time in the correct quadrant than did TsVeh (Kruskal-Wallis rank test, $P = 0.001$; Mann-Whitney pairwise comparison, TsVeh versus TsSAG and TsVeh versus EuVeh, $P = 0.001$ and 0.0001 , respectively). (D) Representative search tracks in the probe test show that impaired search strategies used by TsVeh mice are corrected in TsSAG. Shown are representative tracks from a mouse of each group. The black box in the northwest quadrant is the former position of the platform.

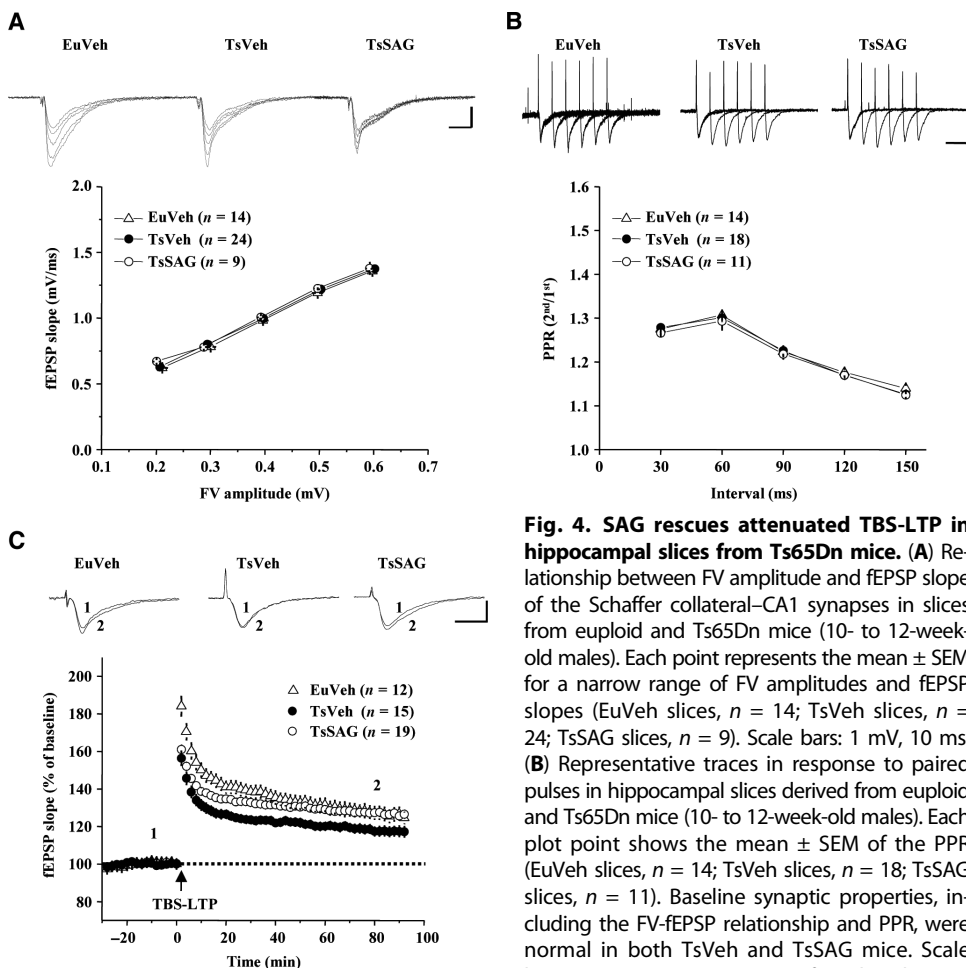


Fig. 4. SAG rescues attenuated TBS-LTP in hippocampal slices from Ts65Dn mice. (A) Relationship between FV amplitude and fEPSP slope of the Schaffer collateral–CA1 synapses in slices from euploid and Ts65Dn mice (10- to 12-week-old males). Each point represents the mean \pm SEM for a narrow range of FV amplitudes and fEPSP slopes (EuVeh slices, $n = 14$; TsVeh slices, $n = 24$; TsSAG slices, $n = 9$). Scale bars: 1 mV, 10 ms. (B) Representative traces in response to paired pulses in hippocampal slices derived from euploid and Ts65Dn mice (10- to 12-week-old males). Each plot point shows the mean \pm SEM of the PPR (EuVeh slices, $n = 14$; TsVeh slices, $n = 18$; TsSAG slices, $n = 11$). Baseline synaptic properties, including the FV-fEPSP relationship and PPR, were normal in both TsVeh and TsSAG mice. Scale bars: 1 mV, 50 ms. (C) SAG significantly enhanced TBS-LTP in slices from Ts65Dn mice. LTP was induced by TBS (five bursts delivered at 5 Hz; each burst consisted of four stimuli at 100 Hz). TBS-induced LTP was significantly reduced in TsVeh ($n = 15$) compared to either EuVeh ($n = 12$) or TsSAG ($n = 19$) (TsVeh versus EuVeh slices: $P = 0.001$ at $t = 30$ min, $P = 0.038$ at $t = 80$ min; TsVeh versus TsSAG slices: $P = 0.006$ at $t = 30$ min, $P = 0.005$ at $t = 80$ min; EuVeh versus TsSAG slices: $P = 0.147$ at 30 min, $P = 0.97$ at $t = 80$ min, compared to EuVeh slices by unpaired two-tailed Student's test). Scale bars: 1 mV, 50 ms.

reduced compared to that in the euploid mice (Fig. 5B and table S15) ($P = 0.06 \pm 0.011$ in Ts65Dn, $n = 11$; $P = 0.39 \pm 0.059$, $n = 13$ in euploid; $P = 0.00002$). The NMDA/AMPA ratio in TsSAG (0.19 ± 0.034 , $n = 11$) was significantly increased compared to that in TsVeh mice ($P = 0.003$) but was not restored to euploid levels ($P = 0.006$). This is consistent with the reduction of NMDAR-dependent LTP in Ts65Dn mice and enhancement of NMDAR-dependent LTP in SAG-treated animals.

DISCUSSION

GCPs in cerebellum of newborn Ts65Dn mice demonstrate a short lag in the initiation of the burst of proliferation relative to euploid (10). Acute SAG treatment stimulates the division of trisomic cells, and here, a single treatment on the day of birth was sufficient to overcome the transient proliferation deficit and normalize cerebellar structure in adult Ts65Dn mice. Ts65Dn mice do not show behavioral measures of cerebellar dysfunction in typical assays such as the accelerating rotarod (8, 35). Accordingly, our analysis focused on electrophysiological measures and revealed that SAG treatment is linked to a modest increase of LTD in lobule III (but not in lobule IX) of Ts65Dn. In contrast, a single treatment with SAG resulted in robust improvement in learning and memory behavior in assays that are sensitive to hippocampal function, and to improved NMDAR function and synaptic plasticity. The persistence of these improvements is striking and invites comparison with reports of persistent improvements of cognition and LTP after pharmacological treatment of adolescent Ts65Dn mice with γ -aminobutyric acid type A (GABA_A) antagonists (36, 37). Understanding the basis for these long-term therapeutic effects may have implications for treating DS, and the current results should encourage further exploration of a possible role for Shh in perinatal programming of hippocampus.

127.3 \pm 3.7% of baseline at $t = 80$ min (Fig. 4C and table S13). TBS-induced LTP in TsVeh was significantly reduced (123.6 \pm 2.3% of baseline at $t = 30$ min, $P = 0.001$) and continued to decay more rapidly than in euploid control mice (117.4 \pm 2.7% of baseline at $t = 80$ min, $P = 0.038$), consistent with previous findings (34). However, in acute hippocampal slices derived from TsSAG mice, the magnitude of TBS-induced LTP was significantly increased compared to TsVeh (132.9 \pm 2.2% of baseline at $t = 30$ min, $P = 0.006$) and not different from euploid (127.4 \pm 2.0% of baseline at $t = 80$ min, $P = 0.97$).

We examined synaptic properties that might underlie reduced LTP in Ts65Dn. The current-voltage relationship of evoked EPSCs in Schaffer collateral–CA1 synapses was similarly linear in euploid and Ts65Dn mice (Fig. 5A and table S14), indicating no difference in calcium-permeable AMPARs. Next, we monitored the amplitude of evoked EPSCs using conditions that separately reveal AMPAR- and N-methyl-D-aspartate receptor (NMDAR)-dependent responses. The ratio of the NMDAR/AMPA-dependent responses in Ts65Dn mice was markedly

SAG penetrates the blood-brain barrier (10, 16, 18) and can be anticipated to activate Shh signaling in cerebellar and hippocampal neurons. We did not see compensation of the small deficit in the number of replicating cells in DG of Ts65Dn by perinatal SAG treatment. From this result, it appears that normalization of DG cell number is not a necessary condition for normalizing the several behavioral and physiological outcomes in Ts65Dn mice that were assessed in this study. Normalization of cerebellar morphology might contribute to improved behavioral outcomes in the MWM. The cerebellum plays an important role in spatial learning, where it is involved in the acquisition of optimal strategies in tasks in which memory is a component,

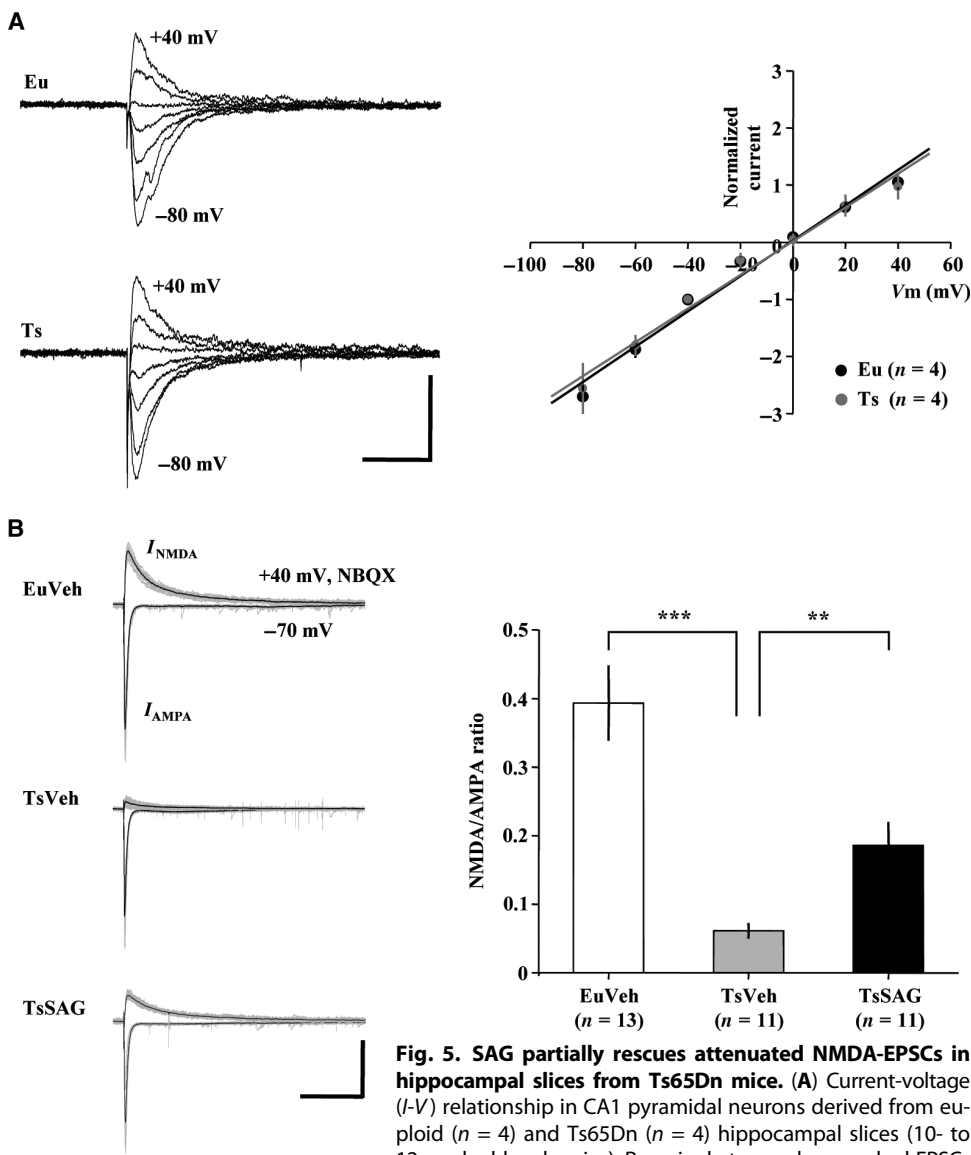


Fig. 5. SAG partially rescues attenuated NMDA-EPSCs in hippocampal slices from Ts65Dn mice. (A) Current-voltage (*I*-*V*) relationship in CA1 pyramidal neurons derived from euploid ($n = 4$) and Ts65Dn ($n = 4$) hippocampal slices (10- to 12-week-old male mice). Raw single traces show evoked EPSCs

obtained while holding postsynaptic cells at membrane potentials ranging from -80 to $+40$ mV in 20-mV steps recorded in the presence of D-AP5 ($50 \mu\text{M}$) and Gabazine ($10 \mu\text{M}$) to isolate AMPAR-mediated EPSCs. For measurement of *I*-*V* curves, spermine ($100 \mu\text{M}$) was added to block GluR2-lacking AMPARs at positive potentials. Graph shows *I*-*V* relationship normalized to the peak EPSC amplitude at -40 mV (V_m indicates membrane potential). The data were fitted by a line giving an estimate for the reversal potential of -0.9 mV (euploid in black) and -0.5 mV (Ts65Dn in gray), respectively (corrected for liquid junction potential). The voltage dependence of the evoked AMPA current was not significantly different between euploid and Ts65Dn. Scale bars: 100 pA, 50 ms. (B) Raw (gray) and averaged (black) traces from a series of 20 consecutive evoked EPSCs recorded from hippocampal Schaffer collateral-CA1 synapses (10- to 12-week-old male mice). Peak AMPA currents were measured at -70 mV, and NMDA currents at $+40$ mV in the presence of 2,3-dihydroxy-6-nitro-7-sulfamoylbenzo[*f*]quinoxaline (NBQX). The NMDA/AMPA ratio was diminished in Ts65Dn neurons ($n = 11$) compared with euploid ($n = 13$). SAG treatment significantly increased NMDA currents in Ts65Dn neurons ($n = 11$). Error bars represent the means \pm SEM (TsVeh versus TsSAG: $P = 0.003$; EuVeh versus TsVeh: $P = 1.7 \times 10^{-5}$; EuVeh versus TsSAG: $P = 0.006$, unpaired two-tailed Student's *t* test). Scale bars: 200 pA, 250 ms.

including the MWM hidden platform (33, 38–42). Here, improved learning and memory were correlated with normalization of cerebellar morphology after SAG treatment. These results are consistent with

a role of cerebellum in spatial learning and suggest that the marked cerebellar hypoplasia in DS may contribute to some cognitive deficits as well.

Up-regulation of the Shh pathway by SAG has now been shown to be efficacious in several situations. In addition to correction of cerebellar hypoplasia in trisomic models, Shh or SAG can support proliferation of neural precursors in vivo after spinal cord injury in rats (43). SAG administration can also counter the antiproliferative effects of glucocorticoids on cerebellar GCPs in newborn mice (17, 43). A number of ciliopathies have pathology related to disruption of hedgehog signaling (44), and SAG might have a therapeutic role in ameliorating some of these effects.

However, pharmacological stimulation of the Shh pathway in newborn infants as a therapeutic strategy might be problematic. Hedgehog signaling plays a central role in many fundamental aspects of development including axis formation and generation of neural crest, and many of its effects are dosage-sensitive. Shh is also required for stem cell generation and maintenance in differentiated tissues. Chronic Shh pathway stimulation is observed in a number of tumor types and directly linked to an increased incidence of medulloblastoma (45, 46). SAG-treated mice studied here showed no evidence of tumor formation or obvious complications in the first 4 months of life. Before a clinical application is contemplated in people with DS, however, it will be necessary to better understand the SAG role in hippocampal function and the sensitivity to possible side effects on different genetic backgrounds while refining both the dosage and the route of drug administration. It would be useful to understand why trisomic GCP (and possibly other trisomic cells) has an attenuated response to the mitogenic effects of Shh, which might offer further targets for therapy (47). We note that there is no evidence in our data and no current theoretical basis for a positive role of Shh pathway stimulation at birth on cognitive ability in euploid adults.

We demonstrated the efficacy of a possible approach to the improvement of learning and memory in a trisomic mouse model.

A single injection of a Shh pathway agonist on the day of birth corrected a key developmental deficiency in cerebellum, restoring normal structure in adults. This single treatment evoked a positive and lasting effect on

hippocampal-dependent learning and memory, and partially normalized hippocampal synaptic NMDAR function and NMDAR-dependent LTP expression. These observations suggest a possible approach to ameliorate cognitive deficits that occur as a consequence of trisomy 21.

MATERIALS AND METHODS

Study design

Our previously published studies show that the Ts65Dn mouse displays and predicts aspects of cerebellar pathology that occur in people with DS, that the cerebellar hypoplasia is substantially due to an attenuated response of gcp to the mitogenic effects of Shh growth factor in the period close to the time of birth, and that stimulation of the Shh pathway with systemic application of SAG at P0 eliminates the gcp deficit at P6 (8, 10). On the basis of these findings, we designed a study to determine whether these effects of SAG might extend beyond the perinatal period. We injected animals at birth with a dose of SAG that produced salutary effects in previous studies from our laboratory and others (10, 16–18). One set of animals was prepared for behavior studies on the basis of our previous determination of variation/cohort size required to power a significant analysis of the MWM paradigm, which is robustly affected in Ts65Dn mice. Similarly, sample sizes for the cohorts subjected to the standard electrophysiological paradigms tested here were chosen on the basis of previous experience. Statistical analyses are described in detail below. In all cases, investigators performing tests were blind to genotype and treatment.

Animals

Founder B6EiC3H-*a/A*-Ts65Dn (Ts65Dn) mice were obtained from the Jackson Laboratory and maintained in our colony as an advanced intercross on a C57BL/6J × C3H/HeJ background.

SAG was synthesized as described (15), dissolved in ethanol or dimethyl sulfoxide, and resuspended in triolein. Activity of this batch of SAG was established by comparison to the amount of GCP proliferation relative to Shh (10, 15) (fig. S1). Each pup in a given litter received a subcutaneous dose of SAG (20 µg/g) or vehicle in 20 µl.

Behavior testing. Animals were given a coded ID by someone other than the investigator so that all tests were performed by investigators who were blind to genotype and treatment group. Tests were performed in the following order: open field, Y maze, MWM. The open-field test was conducted in the photobeam activity system (San Diego Instruments) in a novel room to which the mice had not been habituated before the test. Mice were placed in a clear acrylic container [16 inches (*W*) × 16 inches (*D*) × 15 inches (*H*)] for 90 min in the first phase and 50 min in the second phase. The numbers of movements at the center, movements at the periphery, and rearings were recorded. Normalized activity is defined as the number of beam breaks at the center or periphery divided by the total number of beam breaks by the mouse. This was further categorized as fine motor activity (if the same beam is broken twice sequentially) or ambulatory activity (if contiguous beams are broken). Data shown are from both phases of open-field testing (table S5).

For the Y maze, mice were habituated to handling for 3 days. They were released on a randomly chosen arm of a stainless steel Y-shaped apparatus, and movements were tracked for 5 min with the SMART program (San Diego Instruments). An entrance was scored when the head and front two paws were in an arm >0.2 s (table S6).

MWM was initiated a week after Y maze (9). A tank of 120-cm diameter was filled with dilute latex paint at 19° to 22°C. For the visible platform test, the position of a platform submerged about 1 cm below the surface was indicated with a flag. This test was conducted on 1 day with three blocks of trials of four attempts each lasting up to 60 s. The position of the cued platform was changed for each attempt in each trial (table S7). The hidden platform test was conducted 10 days later, with the platform always in the same position for three training days. Latency and path were recorded (table S8). The following day, the platform was removed for the probe trial, when mice were allowed to swim for 3 min and the time spent in each quadrant was measured (table S9). Tracks followed by the mice were extracted with the SMART program (San Diego Instruments) and scored with a modification of the method of Petrosini *et al.* (38) (fig. S4 and table S10).

Histological measurements. Tissue harvest and histological preparation were performed as described (8). Relative midline sagittal area of the cerebellum was measured with ImageJ and normalized to the midline area of the entire brain. Unbiased stereology was performed with Stereologer 1.3 (SPA Inc.) on 30-µm sections of the brain of P6 animals. The optical disector method was used to obtain density, and Cavalieri's principle was used to estimate volume (48). The frame area of the disectors was 169 µm², depth was 10 µm, and guard height was 5 µm. Disectors were spaced at intervals of 95 µm. Nuclei were counted at 500×. The coefficient of error within and between samples was ≤10%. The sampling fraction was one in six sections. On average, 13 sections per animal were sampled.

BrdU (250 mg/g) was included in the SAG or vehicle preparations injected at P0. Treated mice were sacrificed at P6. The brain was fixed in 4% paraformaldehyde for 14 hours at 4°C and then transferred to 20% sucrose solution with one change after 24 hours. Serial coronal sections (50 µm) that contained the hippocampus were cut from lateral 1.94 mm to –4.04 mm bregma, compare the Mouse Brain in Stereotaxic Coordinates (46). One in five sections was processed for BrdU and NeuN double labeling according to the indirect immunofluorescence method of Coons (47) with the primary mouse anti-NeuN biotin (Chemicon) and rat anti-BrdU (Novus) antibodies, followed by secondary Alexa Fluor 488 donkey anti-rat immunoglobulin G (IgG) (Molecular Probes) and Alexa Fluor 594 streptavidin (Molecular Probes) antibodies. The number of BrdU-labeled nuclei in the DG was estimated with the principles of unbiased stereology as described above. Volume (V_{ref}) of the chosen half of the DG was estimated with the total area of the sampled sections (A_{ref}), the average thickness of the sections (t), and the sampling fraction. Each sampled section was imaged with two-photon excitation by the Chameleon Vision II laser (Coherent Inc.) attached to a Zeiss axiscope 710NLO microscope. A low-magnification image was used to determine the section area. A pilot experiment determined the area and density of the optical disector placement so as to allow counting of about 15 to 20 nuclei per section or 100 to 150 nuclei per animal. On average, eight sections were analyzed per animal. An area of 21 µm × 21 µm was found to be acceptable with one disector placed every 0.02 mm² through the DG. An estimate of the total number of BrdU-labeled nuclei was attained by multiplying the V_{ref} by N_v (observed density) (tables S2 and S3).

Electrophysiology

Cerebellum. Parasagittal slices (250 µm) were obtained from EuVeh ($n = 9$), EuSAG ($n = 5$), TsVeh ($n = 9$), or TsSAG ($n = 9$) mice aged

21 to 28 days with a Leica vibratome in an ice-cold cutting solution containing 225 mM sucrose, 119 mM NaCl, 2.5 mM KCl, 0.1 mM CaCl_2 , 4.9 mM MgCl_2 , 26.2 mM NaHCO_3 , 1 mM NaH_2PO_4 , 1.25 mM glucose, and 3 mM kynurenic acid bubbled with 95% O_2 and 5% CO_2 . Whole-cell recordings were made from Purkinje cells in either lobule III or lobule IX at -70 mV in artificial cerebrospinal fluid (aCSF) containing 124 mM NaCl, 2.5 mM KCl, 2.5 mM CaCl_2 , 1.3 mM MgCl_2 , 26.2 mM NaHCO_3 , 1 mM NaH_2PO_4 , and 20 mM glucose bubbled with 95% O_2 and 5% CO_2 at room temperature. Gabazine (5 μM) (Sigma) was added to block GABA_A receptor currents. Recording electrodes contained a solution composed of 120 mM Cs-methanesulfonate, 10 mM CsCl, 10 mM Hepes, 0.2 mM EGTA, 4 mM $\text{Na}_2\text{-ATP}$ (adenosine triphosphate), and 0.4 mM Na-GTP (guanosine triphosphate) (pH 7.25). Paired stimulations (50 ms apart) were done with a glass electrode filled with aCSF by passing 20 to 40 μA of current with 0.2-ms duration to evoke EPSCs having around 200-pA amplitude. LTD was induced by a train of 10 stimuli at 100 Hz depolarizing the postsynaptic cells to 0 mV, which was repeated 30 times every 2 s. Currents were filtered at 1 kHz, measured with Multiclamp 700B (Molecular Devices), and acquired with Clampex software (Molecular Devices) at 5 kHz. EPSC amplitudes, rise time, and decay tau were measured offline with Clampfit software (Molecular Devices). Two-way ANOVA was used for statistical analysis (table S4).

Hippocampus: Slice preparation. Transverse hippocampal slices (400- μm thick) were prepared at P90 to P120 by cutting on a tissue slicer in ice-cold dissection buffer: 110 mM choline chloride, 2.5 mM KCl, 7 mM MgCl_2 , 0.5 mM CaCl_2 , 2.4 mM sodium pyruvate, 1.3 mM sodium L-ascorbate, 1.2 mM NaH_2PO_4 , 25 mM NaHCO_3 , and 20 mM D-glucose. Slices were recovered for 3 to 6 hours at room temperature in aCSF composed of 124 mM NaCl, 2.5 mM KCl, 1.3 mM MgCl_2 , 2.5 mM CaCl_2 , 1 mM NaH_2PO_4 , 26.2 mM NaHCO_3 , and 20 mM D-glucose and saturated with 95% O_2 and 5% CO_2 . Hemislices were recorded in an interface chamber, maintained at 32°C for 1 hour, and perfused continuously with aCSF at a rate of 3 ml/min.

Hippocampus: Field potential recording. fEPSPs were recorded from the stratum radiatum of acute hippocampal slices in response to stimulation of the Schaffer collateral–commissural pathway, as described (49). Stimulus intensity was adjusted to elicit 50 to 60% of the maximal fEPSP slope response. LTP was measured in Schaffer collateral–CA1 synapses. Experimenters were blind to the genotype/treatment throughout the experiments. LTP was induced by TBS (five trains of four pulses; at 100 Hz and 200 ms apart). Evoked responses were stored online and analyzed offline with Clampfit (version 9.2). Time course of LTP was expressed as percentage of the fEPSP slope during the baseline recording (tables S11 to S13).

NMDAR/AMPA ratio and *I-V* curves of AMPA-evoked EPSCs

Evoked EPSCs and the peak amplitude were recorded at a holding potential of $V_h = -70$ mV to access AMPAR-mediated responses. NMDAR-mediated responses were next recorded at $V_h = +40$ mV in the presence of the selective AMPAR antagonist NBQX (10 mM, Tocris). For *I-V* curves, spermine (100 μM , Sigma) was added to the pipette solution to block GluR2-lacking AMPARs at positive potentials. Evoked AMPAR-mediated responses were recorded from different membrane potentials ranging from -80 to $+40$ mV in 20-mV steps. Amplitudes of currents were normalized to the value measured at -40 mV. Whole-cell voltage-clamp recordings of hippocampal CA1 pyramidal neurons were performed in the presence of GABA_A receptor antagonist (10 mM

Gabazine, Sigma) and NMDAR antagonist (50 mM D-AP5, Sigma). The pipette solution contained 90 mM Cs-methanesulfonate, 48.5 mM CsCl, 5 mM EGTA, 2 mM MgCl_2 , 2 mM Na-ATP, 0.4 mM Na-GTP, 1 mM QX 314 bromide, and 5 mM Hepes (pH 7.2, 290 ± 5 mmol/kg). Statistical comparison was performed by the independent *t* test and ANOVA for multiple comparisons (tables S14 and S15).

Statistical analysis

All statistical tests were conducted in SPSS or SigmaStat. All analyses presented here were performed specifically to compare TsVeh, TsSAG, and EuVeh. In all instances where EuSAG data are reported, they are always compared to the EuVeh group in a pairwise analysis with Fisher's LSD. All behavioral tests were performed while the experimenter was blinded to genotype and treatment. Statistical analyses were similarly conducted blinded to genotype and treatment.

All morphological data (cell number, density, and areas) were tested for normality by quantile-quantile plots or Kolmogorov-Smirnov test. MANOVA (Wilk's λ) was carried out for cerebellar GC density and normalized area, followed by pairwise comparisons with Fisher's LSD. For GC number in the P6 DG, pairwise comparisons between the three groups were carried out with Fisher's LSD. Normalized numbers of BrdU-labeled cells in the GC were analyzed with one-way ANOVA followed by Fisher's LSD. Open-field data were tested with MANOVA for normalized number of fine motor and ambulatory movements at the center versus the periphery and for the number of rearings and for spontaneous alternation and number of arm entries in the Y maze. The value of Wilk's λ was determined, followed by correction for multiple pairwise comparisons with the Bonferroni method. All MWM data were tested for normal distribution with Kolmogorov-Smirnov test or quantile-quantile plots. The hidden platform data were transformed before being tested in parametric tests. The probe test data and strategy scores were analyzed with nonparametric tests. Latency to platform in the MWM was analyzed with two-way repeated-measures ANOVA, with the trials in visible or hidden platform included as the repeated measurement, followed by multiple pairwise comparisons between the three groups. *P* values were corrected by the Bonferroni method to maintain the family-wise α value at 0.05.

Probe test results in MWM were analyzed with the nonparametric version of one-way ANOVA Kruskal-Wallis rank test, followed by the Mann-Whitney test for pairwise comparisons. Correlation between scores on trajectory and latency was determined with the nonparametric Spearman's rho. The frequency of different scores was compared with the χ^2 test and Fisher's exact *P* value.

SUPPLEMENTARY MATERIALS

www.sciencetranslationalmedicine.org/cgi/content/full/5/201/2011ra120/DC1 Notes

- Fig. S1. SAG had mitogenic activity in primary GCP cultures.
- Fig. S2. Dentate gyrus is not affected by SAG treatment.
- Fig. S3. SAG treatment does not affect open-field performance.
- Fig. S4. SAG treatment does not improve Y maze performance in Ts65Dn mice.
- Fig. S5. SAG treatment normalizes search strategies of Ts65Dn mice in the MWM.
- Table S1. Cerebellar morphological measurements.
- Table S2. Dentate gyrus granule cell number at P6 (hematoxylin-stained).
- Table S3. BrdU-positive cells in the DG at P6.
- Table S4. Electrophysiological measurements from cerebellar Purkinje cells.
- Table S5. Open-field activity.
- Table S6. Total number of entries and percent alternation in Y maze.
- Table S7. Latency in the MWM visible platform test (seconds).

Table S8. Latency in the MWM hidden platform test (seconds).
 Table S9. Time spent in the correct quadrant in the MWM probe test (seconds).
 Table S10. Strategy scores of animals in hidden platform test, by day and trial number.
 Table S11. Relationship between FV amplitude and fEPSP slope.
 Table S12. Paired pulse ratio.
 Table S13. TBS-LTP enhanced by SAG in slices from Ts65Dn mice.
 Table S14. Current-voltage relationship.
 Table S15. NMDA/AMPA ratio.

REFERENCES AND NOTES

- S. E. Antonarakis, R. Lyle, E. T. Dermitzakis, A. Reymond, S. Deutsch, Chromosome 21 and Down syndrome: From genomics to pathophysiology. *Nat. Rev. Genet.* **5**, 725–738 (2004).
- I. Das, R. H. Reeves, The use of mouse models to understand and improve cognitive deficits in Down syndrome. *Dis. Model. Mech.* **4**, 596–606 (2011).
- J. Braudeau, B. Delatour, A. Duchon, P. L. Pereira, L. Dauphinot, F. de Chaumont, J. C. Olivo-Marin, Á. Pazos, J. Flórez, R. Gasser, A. W. Thomas, M. Honer, F. Knoflach, J. L. Trejo, J. G. Wettstein, M. C. Hernández, Reducing GABA_A α 5 receptor-mediated inhibition rescues functional and neuromorphological deficits in a mouse model of Down syndrome. *J. Psychopharmacol.* **25**, 1030–1042 (2011).
- C. Martínez-Cué, P. Martínez, N. Rueda, R. Vidal, S. García, V. Vidal, A. Corrales, J. A. Montero, Á. Pazos, J. Flórez, R. Gasser, A. W. Thomas, M. Honer, F. Knoflach, J. L. Trejo, J. G. Wettstein, M. C. Hernández, Reducing GABA_A α 5 receptor-mediated inhibition rescues functional and neuromorphological deficits in a mouse model of Down syndrome. *J. Neurosci.* **33**, 3953–3966 (2013).
- R. H. Reeves, C. C. Garner, A year of unprecedented progress in Down syndrome basic research. *Ment. Retard. Dev. Disabil. Res. Rev.* **13**, 215–220 (2007).
- A. Ruparella, M. L. Pearn, W. C. Mobley, Cognitive and pharmacological insights from the Ts65Dn mouse model of Down syndrome. *Curr. Opin. Neurobiol.* **22**, 880–886 (2012).
- L. Crome, V. Cowie, E. Slater, A statistical note on cerebellar and brain-stem weight in Mongolism. *J. Ment. Def. Res.* **10**, 69–72 (1966).
- L. L. Baxter, T. H. Moran, J. T. Richtsmeier, J. Troncoso, R. H. Reeves, Discovery and genetic localization of Down syndrome cerebellar phenotypes using the Ts65Dn mouse. *Hum. Mol. Genet.* **9**, 195–202 (2000).
- L. E. Olson, R. J. Roper, L. L. Baxter, E. J. Carlson, C. J. Epstein, R. H. Reeves, Down syndrome mouse models Ts65Dn, Ts1Cje, and Msi1Cje/Ts65Dn exhibit variable severity of cerebellar phenotypes. *Dev. Dyn.* **230**, 581–589 (2004).
- R. J. Roper, L. L. Baxter, N. G. Saran, D. K. Klindinst, P. A. Beachy, R. H. Reeves, Defective cerebellar response to mitogenic Hedgehog signaling in Down's syndrome mice. *Proc. Natl. Acad. Sci. U.S.A.* **103**, 1452–1456 (2006).
- S. Trazzi, V. M. Mitrugno, E. Valli, C. Fuchs, S. Rizzi, S. Guidi, G. Perini, R. Bartesaghi, E. Ciani, APP-dependent up-regulation of Ptch1 underlies proliferation impairment of neural precursors in Down syndrome. *Hum. Mol. Genet.* **20**, 1560–1573 (2011).
- V. A. Wallace, Purkinje-cell-derived Sonic hedgehog regulates granule neuron precursor cell proliferation in the developing mouse cerebellum. *Curr. Biol.* **9**, 445–448 (1999).
- N. Dahmane, A. Ruiz-i-Altaba, Sonic hedgehog regulates the growth and patterning of the cerebellum. *Development* **126**, 3089–3100 (1999).
- R. J. Wechsler-Reya, M. P. Scott, Control of neuronal precursor proliferation in the cerebellum by Sonic hedgehog. *Neuron* **22**, 103–114 (1999).
- J. K. Chen, J. Taipale, K. E. Young, T. Maiti, P. A. Beachy, Small molecule modulation of Smoothed activity. *Proc. Natl. Acad. Sci. U.S.A.* **99**, 14071–14076 (2002).
- M. Frank-Kamenetsky, X. M. Zhang, S. Bottega, O. Guicherit, H. Wichterle, H. Dudek, D. Bumcrot, F. Y. Wang, S. Jones, J. Shulok, L. L. Rubin, J. A. Porter, Small-molecule modulators of Hedgehog signaling: Identification and characterization of Smoothed agonists and antagonists. *J. Biol.* **1**, 10 (2002).
- V. M. Heine, A. Griveau, C. Chapin, P. L. Ballard, J. K. Chen, D. H. Rowitch, A small-molecule Smoothed agonist prevents glucocorticoid-induced neonatal cerebellar injury. *Sci. Transl. Med.* **3**, 105ra104 (2011).
- R. Machold, S. Hayashi, M. Rutlin, M. D. Muzumdar, S. Nery, J. G. Corbin, A. Gritti-Linde, T. Dellovade, J. A. Porter, L. L. Rubin, H. Dudek, A. P. McMahon, G. Fishell, Sonic hedgehog is required for progenitor cell maintenance in telencephalic stem cell niches. *Neuron* **39**, 937–950 (2003).
- A. Salehi, J. D. Delcroix, P. V. Belichenko, K. Zhan, C. Wu, J. S. Valletta, R. Takimoto-Kimura, A. M. Kleschevnikov, K. Sambamurti, P. P. Chung, W. Xia, A. Villar, W. A. Campbell, L. S. Kulnane, R. A. Nixon, B. T. Lamb, C. J. Epstein, G. B. Stokin, L. S. Goldstein, W. C. Mobley, Increased *App* expression in a mouse model of Down's syndrome disrupts NGF transport and causes cholinergic neuron degeneration. *Neuron* **51**, 29–42 (2006).
- A. M. Insausti, M. Megias, D. Crespo, L. M. Cruz-Orive, M. Dierssen, I. F. Vallina, R. Insausti, J. Flórez, Hippocampal volume and neuronal number in Ts65Dn mice: A murine model of Down syndrome. *Neurosci. Lett.* **253**, 175–178 (1998).
- H. A. Lorenzi, R. H. Reeves, Hippocampal hypocellularity in the Ts65Dn mouse originates early in development. *Brain Res.* **1104**, 153–159 (2006).
- L. Chakrabarti, Z. Galdzicki, T. F. Haydar, Defects in embryonic neurogenesis and initial synapse formation in the forebrain of the Ts65Dn mouse model of Down syndrome. *J. Neurosci.* **27**, 11483–11495 (2007).
- P. V. Belichenko, E. Maslah, A. M. Kleschevnikov, A. J. Villar, C. J. Epstein, A. Salehi, W. C. Mobley, Synaptic structural abnormalities in the Ts65Dn mouse model of Down syndrome. *J. Comp. Neurol.* **480**, 281–298 (2004).
- B. F. Pennington, J. Moon, J. Edgin, J. Stedron, L. Nadel, The neuropsychology of Down syndrome: Evidence for hippocampal dysfunction. *Child Dev.* **74**, 75–93 (2003).
- R. H. Reeves, N. G. Irving, T. H. Moran, A. Wohn, C. Kitt, S. S. Sisodia, C. Schmidt, R. T. Bronson, M. T. Davison, A mouse model for Down syndrome exhibits learning and behaviour deficits. *Nat. Genet.* **11**, 177–184 (1995).
- R. J. Siarey, E. J. Coan, S. I. Rapoport, Z. Galdzicki, Responses to NMDA in cultured hippocampal neurons from trisomy 16 embryonic mice. *Neurosci. Lett.* **232**, 131–134 (1997).
- A. M. Kleschevnikov, P. V. Belichenko, A. J. Villar, C. J. Epstein, R. C. Malenka, W. C. Mobley, Hippocampal long-term potentiation suppressed by increased inhibition in the Ts65Dn mouse, a genetic model of Down syndrome. *J. Neurosci.* **24**, 8153–8160 (2004).
- J. E. Hanson, M. Blank, R. A. Valenzuela, C. C. Garner, D. V. Madison, The functional nature of synaptic circuitry is altered in area CA3 of the hippocampus in a mouse model of Down's syndrome. *J. Physiol.* **579**, 53–67 (2007).
- J. R. Epp, M. D. Spritzer, L. A. Galea, Hippocampus-dependent learning promotes survival of new neurons in the dentate gyrus at a specific time during cell maturation. *Neuroscience* **149**, 273–285 (2007).
- E. Gould, P. Tanapat, T. Rydel, N. Hastings, Regulation of hippocampal neurogenesis in adulthood. *Biol. Psychiatry* **48**, 715–720 (2000).
- C. H. Kim, S. H. Oh, J. H. Lee, S. O. Chang, J. Kim, S. J. Kim, Lobule-specific membrane excitability of cerebellar Purkinje cells. *J. Physiol.* **590**, 273–288 (2012).
- M. M. Usowicz, C. L. Garden, Increased excitability and altered action potential waveform in cerebellar granule neurons of the Ts65Dn mouse model of Down syndrome. *Brain Res.* **1465**, 10–17 (2012).
- E. Burguière, A. Arleo, M. R. Hojjati, Y. Elgersma, C. I. De Zeeuw, A. Berthoz, L. Rondi-Reig, Spatial navigation impairment in mice lacking cerebellar LTD: A motor adaptation deficit? *Nat. Neurosci.* **8**, 1292–1294 (2005).
- A. C. Costa, M. J. Grybko, Deficits in hippocampal CA1 LTP induced by TBS but not HFS in the Ts65Dn mouse: A model of Down syndrome. *Neurosci. Lett.* **382**, 317–322 (2005).
- L. A. Hyde, L. S. Crnic, A. Pollock, P. C. Bickford, Motor learning in Ts65Dn mice, a model for Down syndrome. *Dev. Psychobiol.* **38**, 33–45 (2001).
- F. Fernandez, W. Morishita, E. Zuniga, J. Nguyen, M. Blank, R. C. Malenka, C. C. Garner, Pharmacotherapy for cognitive impairment in a mouse model of Down syndrome. *Nat. Neurosci.* **10**, 411–413 (2007).
- A. M. Kleschevnikov, P. V. Belichenko, M. Faizi, L. F. Jacobs, K. Htun, M. Shamloo, W. C. Mobley, Deficits in cognition and synaptic plasticity in a mouse model of Down syndrome ameliorated by GABA_B receptor antagonists. *J. Neurosci.* **32**, 9217–9227 (2012).
- L. Petrosini, M. G. Leggio, M. Molinari, The cerebellum in the spatial problem solving: A co-star or a guest star? *Prog. Neurobiol.* **56**, 191–210 (1998).
- E. Burguière, A. Arabo, F. Jarlier, C. I. De Zeeuw, L. Rondi-Reig, Role of the cerebellar cortex in conditioned goal-directed behavior. *J. Neurosci.* **30**, 13265–13271 (2010).
- R. Feil, J. Hartmann, C. Luo, W. Wolfgruber, K. Schilling, S. Feil, J. J. Barski, M. Meyer, A. Konnerth, C. I. De Zeeuw, F. Hofmann, Impairment of LTD and cerebellar learning by Purkinje cell-specific ablation of cGMP-dependent protein kinase I. *J. Cell Biol.* **163**, 295–302 (2003).
- Z. Gao, B. J. van Beugen, C. I. De Zeeuw, Distributed synergistic plasticity and cerebellar learning. *Nat. Rev. Neurosci.* **13**, 619–635 (2012).
- M. Schonewille, Z. Gao, H. J. Boele, M. F. Veloz, W. E. Amerika, A. A. Simek, M. T. De Jeu, J. P. Steinberg, K. Takamiya, F. E. Hoebeek, D. J. Linden, R. L. Huganir, C. I. De Zeeuw, Reevaluating the role of LTD in cerebellar motor learning. *Neuron* **70**, 43–50 (2011).
- N. C. Bambakidis, X. Wang, R. J. Lukas, R. F. Spetzler, V. K. Sonntag, M. C. Preul, Intravenous hedgehog agonist induces proliferation of neural and oligodendrocyte precursors in rodent spinal cord injury. *Neurosurgery* **67**, 1709–1715 (2010).
- J. van Rееuwijk, H. H. Arts, R. Roepman, Scrutinizing ciliopathies by unraveling ciliary interaction networks. *Hum. Mol. Genet.* **20**, R149–R157 (2011).
- L. V. Goodrich, L. Milenković, K. M. Higgins, M. P. Scott, Altered neural cell fates and medulloblastoma in mouse patched mutants. *Science* **277**, 1109–1113 (1997).
- G. J. Weiss, R. L. Korn, Metastatic basal cell carcinoma in the era of hedgehog signaling pathway inhibitors. *Cancer* **118**, 5310–5319 (2012).
- D. G. Currier, R. C. Polk, R. H. Reeves, in *Progress in Brain Research*, M. Dierssen, R. De La Torre, Eds. (Elsevier, London, 2012), vol. 197, pp. 223–236.
- P. R. Mouton, *Principles and Practices of Unbiased Stereology: An Introduction for Bioscientists* (The Johns Hopkins University Press, Baltimore, 2002), p. 214.

49. S. Park, J. M. Park, S. Kim, J. A. Kim, J. D. Shepherd, C. L. Smith-Hicks, S. Chowdhury, W. Kaufmann, D. Kuhl, A. G. Ryazanov, R. L. Huganir, D. J. Linden, P. F. Worley, Elongation factor 2 and fragile X mental retardation protein control the dynamic translation of Arc/Arg3.1 essential for mGluR-LTD. *Neuron* **59**, 70–83 (2008).

Acknowledgments: We thank D. J. Meyers (Johns Hopkins University School of Medicine Synthetic Core Facility) for the synthesis of SAG 1.1, which was supported in part by a grant from the Flight Attendant Medical Research Institute. **Funding:** This work was supported by the Down Syndrome Research and Treatment Foundation, Research Down Syndrome, and R01 HD38384 from the National Institute of Child Health and Human Development (R.H.R.); the intramural programs of National Institute on Alcohol Abuse and Alcoholism at the NIH (J.H.S.); MH51106 from the National Institute of Mental Health (D.J.L.); and R01 NS39156 from the National Institute of Neurological Diseases and Stroke (P.F.W.). The information presented does not necessarily reflect the opinions of the funding agencies. **Author contributions:** I.D. performed and analyzed anatomical data and behavioral experiments with R.H.R. J.-M.P. performed hippocampal electrophysiology and analyzed the data with D.J.L. and P.F.W. J.H.S. performed the cerebellar

electrophysiology and analyzed the data with D.J.L. and P.F.W. H.L. performed stereology on P6 DG and analyzed the data with R.H.R. I.D. and R.H.R. designed the overall study and wrote the manuscript. All authors contributed to the manuscript. R.H.R. conceived and coordinated the project. **Competing interests:** The authors declare that they have no competing interests. R.H.R. is a member of Science Advisory Boards of the Down Syndrome Research and Treatment Foundation, Research Down Syndrome, the Linda Crnic Institute, and the National Down Syndrome Society; none of these positions are remunerated.

Submitted 21 February 2013

Accepted 8 July 2013

Published 4 September 2013

10.1126/scitranslmed.3005983

Citation: I. Das, J.-M. Park, J. H. Shin, S. K. Jeon, H. Lorenzi, D. J. Linden, P. F. Worley, R. H. Reeves, Hedgehog agonist therapy corrects structural and cognitive deficits in a Down syndrome mouse model. *Sci. Transl. Med.* **5**, 201ra120 (2013).

Hedgehog Agonist Therapy Corrects Structural and Cognitive Deficits in a Down Syndrome Mouse Model

Ishita Das, Joo-Min Park, Jung H. Shin, Soo Kyeong Jeon, Hernan Lorenzi, David J. Linden, Paul F. Worley and Roger H. Reeves

Sci Transl Med 5, 201ra120201ra120.
DOI: 10.1126/scitranslmed.3005983

Sonic Hedgehog to the Rescue

Down syndrome, or trisomy 21, is one of the most common chromosomal abnormalities and a common cause of intellectual disability. Although there is no way to correct the underlying genetic abnormality in this disease, the abnormalities in brain structure resulting from the chromosomal change may not be so immutable, according to a new study by Das *et al.*

The authors used a mouse model of Down syndrome to demonstrate that a single dose of a drug that stimulates a signaling pathway called Sonic hedgehog, given shortly after birth, had a number of effects on the mice. The medication improved brain development in treated animals, leading to normalization of cerebellar morphology and some improvement of hippocampal synaptic function by adulthood. Treated mice also exhibited stronger performance on a variety of cognitive tasks involving learning and memory, with results that were often indistinguishable from those of control mice.

The findings of this paper do not imply an imminent cure for Down syndrome or a treatment for human patients in the near future. The effects of Sonic hedgehog on brain development in humans are not yet fully understood, and overactivation of this pathway has been linked to some diseases. Nevertheless, this study provides insights into the biology of Down syndrome and its molecular underpinnings, which may eventually lead to improved therapies for human patients.

ARTICLE TOOLS

<http://stm.sciencemag.org/content/5/201/201ra120>

SUPPLEMENTARY MATERIALS

<http://stm.sciencemag.org/content/suppl/2013/08/30/5.201.201ra120.DC1>

RELATED CONTENT

<http://stm.sciencemag.org/content/scitransmed/1/7/7ra17.full>
<http://stm.sciencemag.org/content/scitransmed/1/7/7ps9.full>
<http://stm.sciencemag.org/content/scitransmed/4/124/124ra29.full>
<http://science.sciencemag.org/content/sci/343/6172/764.full>
<http://science.sciencemag.org/content/sci/343/6174/964.full>
<http://stke.sciencemag.org/content/sigtrans/8/394/ra92.full>
<http://stm.sciencemag.org/content/scitransmed/8/344/344ra85.full>
<http://science.sciencemag.org/content/sci/362/6416/eaau1810.full>
<http://science.sciencemag.org/content/sci/366/6467/797.full>
<http://science.sciencemag.org/content/sci/366/6467/843.full>

REFERENCES

This article cites 47 articles, 12 of which you can access for free
<http://stm.sciencemag.org/content/5/201/201ra120#BIBL>

Use of this article is subject to the [Terms of Service](#)

Science Translational Medicine (ISSN 1946-6242) is published by the American Association for the Advancement of Science, 1200 New York Avenue NW, Washington, DC 20005. The title *Science Translational Medicine* is a registered trademark of AAAS.

Copyright © 2013, American Association for the Advancement of Science

PERMISSIONS

<http://www.sciencemag.org/help/reprints-and-permissions>

Use of this article is subject to the [Terms of Service](#)

Science Translational Medicine (ISSN 1946-6242) is published by the American Association for the Advancement of Science, 1200 New York Avenue NW, Washington, DC 20005. The title *Science Translational Medicine* is a registered trademark of AAAS.

Copyright © 2013, American Association for the Advancement of Science